Energy sharing in the deexcitation of the ^{90}Ru compound nucleus via the $p\alpha$ channel

F. Bourgine, D. Cabaussel, D. Boivin, M. Aïche, M.-M. Aléonard, G. Barreau, J.-F. Chemin, T. P. Doan, J. P. Goudour, M. Harston, and J.-N. Scheurer
Centre d'Etudes Nucléaires de Bordeaux-Gradignan, IN2P3-CNRS, Université Bordeaux I, BP 120, F-33175 Gradignan Cedex, France

A. Brondi, G. La Rana, R. Moro, A. Principe, and E. Vardaci
Dipartimento di Scienze Fisiche dell'Università and Istituto Nazionale di Fisica Nucleare, Mostra d'Oltremare, Pad. 20, I-80125, Napoli, Italy

D. Curien
Institut de Recherches Subatomiques, BP 20, F-67037, Strasbourg Cedex 2, France
(Received 25 February 1997; revised manuscript received 30 July 1997)

Using the 4π light charged-particle detector DIAMANT in combination with the γ-ray spectrometer EUROGAM II, the decay of the ^{90}Ru compound nucleus via the $p\alpha$ channel was studied. These nuclei were produced at an excitation energy of 54.9 MeV and with a maximum angular momentum of $37\hbar$ by the 120 MeV ^{32}S + ^{58}Ni reaction. The measurement of the energy of the two particles allowed the determination of the energy distribution of the entry states. A particular behavior of the sharing of the available energy between the two particles was found: For increasing values of the entry-state energy, the mean energy for protons remains almost constant while for alpha particles it decreases. This behavior is well reproduced by the evaporation code LILITA_N95. The physics underlying the decay is discussed in the framework of the statistical model which predicts a strong correlation between the excitation energy and the angular momentum of the evaporation residue. This result encourages the use of the $p\alpha$ channel to select the excitation energy and the angular momentum of the evaporation residue for superdeformed band studies. [S0556-2813(97)01612-9]

PACS number(s): 25.70.Gh, 23.20.En

I. INTRODUCTION

Much work has been devoted to the study of the properties and the decay of the composite systems, using as probes light particles and γ rays. The statistical model (SM) provided the guidance for data interpretation, allowing extraction of the leading physical quantities such as temperature, angular momentum, and deformation of the emitting system. Most of the studies were based on inclusive measurements of proton, deuteron, triton, and alpha particle energy spectra and angular distributions [1]. More recently, the availability of high efficiency detectors for light charged particles and γ rays provided the opportunity to select decay channels even with low cross sections, allowing extraction of more detailed information on the composite system decay. In particular, the channels involving one or two particles are rather interesting as they provide a stringent test of the statistical model, the decay not being integrated over many particle emission steps. Since these channels involve high spin states of the composite system, the effects of the angular momentum on the decay are expected to be relatively strong. In this respect, the study of these channels provides insights into the level density at high angular momenta for which only a few studies on the basis of very exclusive data have been carried out [2]. Furthermore, particles emitted from the compound nucleus (CN) at high angular momenta are of great interest in the study of the deformed bands. Recent experiments [3] have shown that charged particle–gamma coincidences may be more effective in the search of hyperdeformed structures. The population mechanism of the superdeformed bands is not yet well understood and it is of great interest to investigate whether the observation of charged particles allows selection of both the excitation energy and the angular momentum of the entry states. This implies the understanding of the decay mechanism of the high spin states of the CN, which can be obtained with less ambiguity in the case of channels involving few nonidentical particles.

In this framework we have undertaken the study of the $p\alpha$ channel of the ^{90}Ru compound nucleus to infer the main characteristics of the decay mechanism. In the following sections we first give a general description of the experiment and data handling. Then, particle energy spectra and particle-particle angular correlations for different values of the entry-state excitation energy are presented and compared with the predictions of the statistical model.

II. EXPERIMENTAL SETUP AND DATA ANALYSIS

The experiment was performed at the VIVITRON accelerator in Strasbourg (France). A 120 MeV ^{32}S beam (currents of the order of 1.5 particle nA) was impinging on a self-supporting ^{58}Ni target (800 μg/cm^2 thick). Charged particles were detected by the DIAMANT multidetector array [4], composed of 54 CsI(Tl) scintillators. The detectors were arranged on ten rings of identical detectors placed at the same angle with respect to the beam direction in a quasi-spherical geometry covering a solid angle equal to 92% of 4π sr. Each scintillator, 3 mm thick, was coupled to a photodiode via a Plexiglas light guide. The external radius of the aluminum scattering chamber housing the detectors was 9.3 cm. Light charged particles were identified by the pulse shape analysis technique. The detectors placed in the forward

TABLE I. Relative cross sections of the observed exit channels in the 120 MeV $^{32}S + ^{58}Ni$ fusion-evaporation reaction.

Exit channel	σ [%]
$2p$ (^{88}Mo)	1.3±0.1
$2pn$ (^{87}Mo)	4.5±0.4
$p\alpha$ (^{85}Nb)	1.2±0.1
2α (^{82}Zr)	0.21±0.02
$3p$ (^{87}Nb)	43±2
$3pn$ (^{86}Nb)	1.7±0.2
$2p\alpha$ (^{84}Zr)	22±1
$p2\alpha$ (^{81}Y)	0.40±0.03
$4p$ (^{86}Zr)	25±1
$3p\alpha$ (^{83}Y)	0.72±0.05
$2p2\alpha$ (^{80}Sr)	0.02±0.01

hemisphere were covered by thin Ta foils of different thicknesses, 15 μm, 10 μm, and 7.5 μm, in order to absorb the elastically scattered particles. Energy thresholds resulting from the identification technique and the absorber insertion were in the range from 3.0 to 3.8 MeV and from 8.8 to 11.7 MeV for protons and alpha particles, respectively. Proton and alpha particle energy calibrations were performed by means of sources and in-beam measurements as described in Ref. [5]. In order to select the reaction channel, the DIAMANT detector was inserted into the γ-ray spectrometer EUROGAM II [6], constituted by 30 tapered and 24 clover escape-suppressed Ge detectors. A total number of 580×10^6 particle-gamma coincidence events requiring a gamma fold greater than 4 and at least one particle were measured.

Eleven evaporative channels, involving at least one light charged particle (proton or alpha particle), were observed. The total yield summed over the identified channels has been taken as the fusion-evaporation cross section because the channels involving only neutron evaporation are negligible in this reaction. This was inferred from the γ-ray spectra built by the events without particle detection. In these spectra we have not observed transitions belonging to the evaporation residues produced by pure neutron channels. Futhermore, SM calculations predict very low cross sections for these channels. The experimental relative intensities for the observed channels have been extracted and are reported in Table I. The decay via the $3p$, $4p$, and $2p\alpha$ channels represents about 90% of the total fusion-evaporation cross section. Two-particle channels are populated with very low intensity (1.2% in the case of $p\alpha$ channel). It is worth noting that the highly efficient setup used in the present experiment allowed us to observe very weak channels such as the $2p2\alpha$ channel (0.02% of the fusion cross section).

The particle energy spectra, the energy distribution of the entry states, and particle-particle angular correlations were extracted for most of the identified channels. The selection of a specific channel was achieved using the following procedure: we first required for each event the number and type of detected particles to correspond to the channel of interest; then single gates were set on discrete γ lines associated with the residual nucleus.

The selection of the $p\alpha$ channel is now described in detail. In Fig. 1 we show the γ-ray spectra built from 10% of the measured events. The γ-ray spectrum obtained without any selection is shown in Fig. 1(a). Most of the lines belong to the strongly populated evaporation residues, i.e., ^{87}Nb ($3p$ channel), ^{86}Zr ($4p$ channel), and ^{84}Zr ($2p\alpha$ channel). Figure 1(b) shows the energy distribution of γ rays in coincidence with one proton and one alpha particle. The 634 keV [$13/2^+ \rightarrow 9/2^+$ (g.s.)] and 841 keV ($17/2^+ \rightarrow 13/2^+$) transitions of the ^{85}Nb nucleus [7] produced by the $p\alpha$ channel are indicated. The strong lines associated with the pure proton channels (i.e., $3p$ and $4p$ channels) have completely disappeared. The pollution by the ^{84}Zr γ rays, produced through the very intense $2p\alpha$ channel (about 20 times greater than the $p\alpha$ channel), is caused by the escape of one of the two protons. In this experiment, the efficiency for proton detection and identification was equal to 67% [8]. In order to obtain the particle spectra relative to the $p\alpha$ channel, gates were set on the 634-keV and 841-keV γ-ray transitions of the ^{85}Nb nucleus in the selected spectrum of Fig. 1(b). Spectra were corrected for the contribution of the Compton background under the peaks.

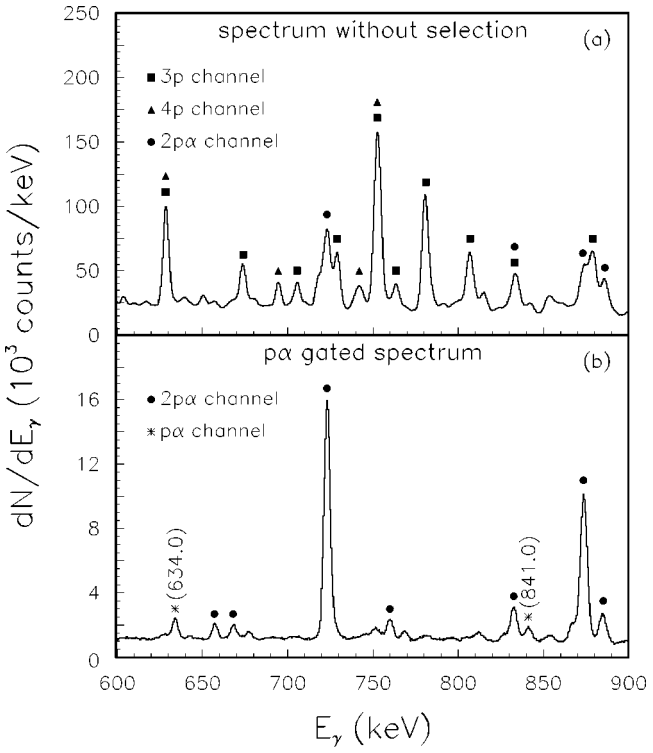

FIG. 1. Gamma-ray energy spectra for the 120 MeV $^{32}S + ^{58}Ni$ reaction. (a) Without any selection. Strong γ lines, associated with the main channels (i.e., $3p$, $4p$, and $2p\alpha$), are indicated. (b) In coincidence with one proton and one alpha particle. Transitions of 634 and 841 keV, belonging to the ^{85}Nb ($p\alpha$ channel), are pointed.

It is worth noting that the selection on the particles greatly improved the peak-to-background ratio in the γ-ray spectra [8], also providing an efficient correction of the Doppler broadening [9]. The selection of very weak channels, with a few percent of the total cross section, required the setting of the above-mentioned stringent conditions to avoid the contamination from other channels. This may explain the relatively small number of studies relating reaction mechanisms and nuclear structure [3,10–12].

Laboratory energy spectra for each particle were obtained

summing over all the detectors belonging to the same ring and requiring the other particle to be detected at any angle in DIAMANT. The energy distribution of the entry states of the evaporation residue in the channel under study was obtained by assigning to each selected event an excitation energy of the entry state given by

$$E_f = E^* - S - E_K^T, \tag{2.1}$$

where E^* is the excitation energy of the compound nucleus, S is the sum of the separation energies of the particles, and E_K^T is the total kinetic energy in the center-of-mass system. This was deduced from the events in which both particles were detected at $\theta_{\rm lab} < 70°$. In this angular range the energy of all emitted particles was higher than the energy thresholds. This choice provided an E_f distribution not affected by the missing events due to the experimental energy threshold. In spite of the low channel cross section and the partial use of DIAMANT we obtained a high quality E_f distribution.

The uncertainty in the E_f values, due to the angular opening of the detectors, varies from 3 to 2 MeV for excitation energies ranging from 5 to 40 MeV. The mean excitation energy of the entry states has been measured by other authors, for several systems, using γ-ray spectrometers [13]. In the case of the Spin Spectrometer used in Refs. [14,15], the uncertainty on E_f varied from 2.3 to 6.5 MeV in the same range of excitation energies as in our system.

Proton-alpha particle azimuthal angular correlations have been extracted for $\theta_{\rm lab} = 57.5°$ (with an angular opening $\Delta\theta = 22.5°$) in the azimuthal angular range from 90° to 180°.

III. STATISTICAL MODEL ANALYSIS OF THE $p\alpha$ CHANNEL AND DISCUSSION

The ^{90}Ru compound nucleus was produced at 54.9 MeV excitation energy. The maximum angular momemtum of the CN, $J_{\rm fus} = 37\hbar$, was deduced in the sharp cutoff approximation from the total fusion cross section measured by Stefanini *et al.* [16]. The particle energy spectra have been analyzed for most of the channels in the framework of the statistical model using the evaporation code LILITA_N95 [17]. This Monte Carlo code was modified to include the experimental conditions such as geometry, energy thresholds, and number of detected particles. A good agreement for all the channels involving more than two particles could be obtained using standard input parameters: a level-density parameter $a = (A/8)$ MeV^{-1}, a rigid-sphere moment of inertia, the optical model transmission coefficients reported in Ref. [18], and a sharp cutoff angular momentum distribution of the CN. The comparison between the experimental spectra and the results of the simulation with these parameters are shown in Fig. 2 for the $3p$, $2pn$, and $2p\alpha$ channels. In the following, we will focus on the $p\alpha$ channel in which case a detailed comparison with the statistical model is possible for both particles.

The measured proton and alpha particle energy spectra in the $p\alpha$ channel at $\theta_{\rm lab} = 57.5°$ are compared to the calculated ones in Fig. 3(a). The latter, corrected by the energy loss in the absorbers, are normalized to the maximum of the experimental spectra in order to compare the shapes. It is worth

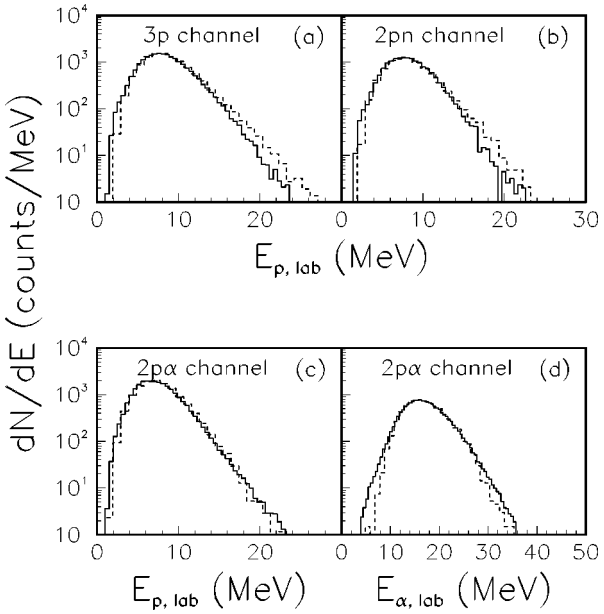

FIG. 2. Measured (solid line) and calculated (dashed line) laboratory energy spectra of protons for the channels (a) $3p$, (b) $2pn$, and (c) $2p\alpha$; of alpha particles for (d) $2p\alpha$ channel.

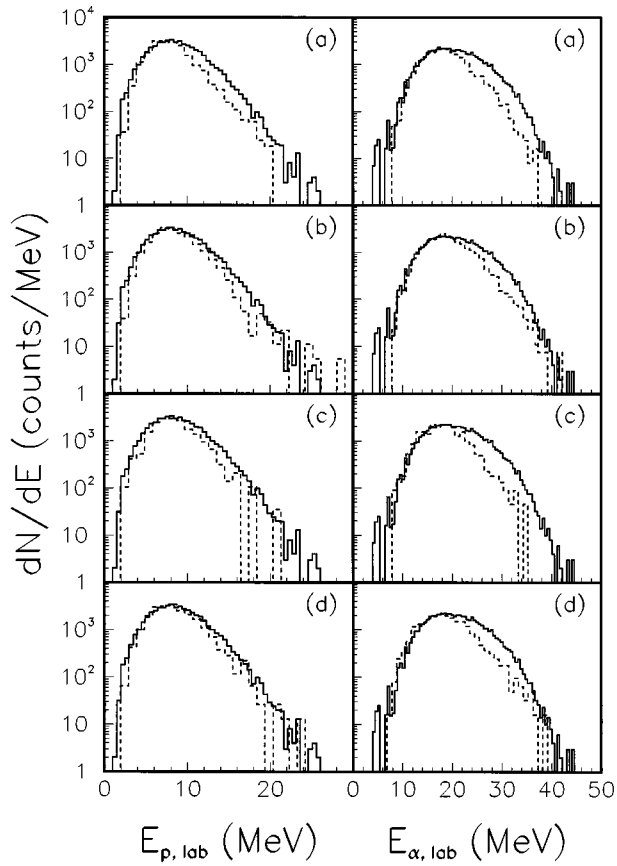

FIG. 3. Measured (solid line) laboratory energy spectra of protons (left) and alpha particles (right) in the $p\alpha$ channel at $\theta_{\rm lab} = 57.5°$, compared with the results of calculations (dashed line): (a) using standard parameters, (b) assuming $a = (A/10)$ MeV^{-1}, (c) with spin-dependent moment of inertia according to the RLDM, and (d) with superdeformed yrast line crossing the spherical yrast line at $J = 28\hbar$.

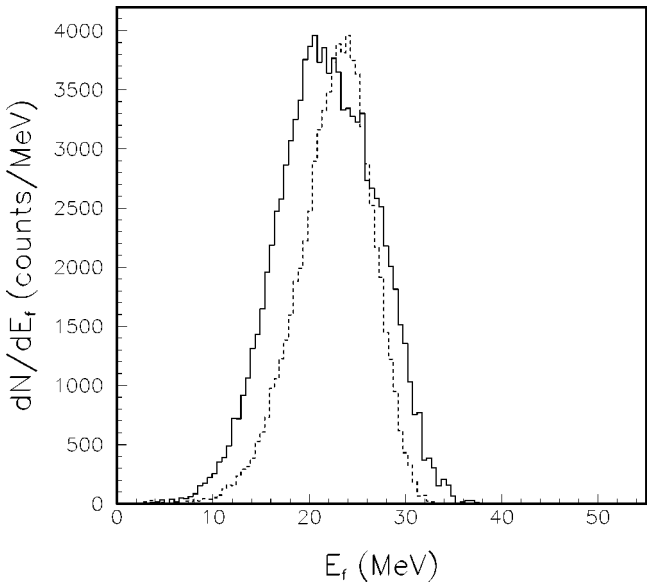

FIG. 4. Measured (solid line) and calculated (dashed line) excitation energy distributions of the evaporation residues E_f for the $p\alpha$ channel.

noting that the alpha-particle spectrum in the $p\alpha$ channel [Fig. 3(a)] differs significantly from the one in the $2p\alpha$ channel. We observe that the simulation underestimates the high energy side of both particle distributions, indicating that the phase space available to this channel is not well accounted for by the model. Several calculations have been carried out changing the relevant parameters of the statistical model. A lower value of the level-density parameter like $(A/10)$ MeV^{-1}, still reasonable at this excitation energy, improves the agreement for the $p\alpha$ channel [Fig. 3(b)], but it makes worse the agreement for the other channels. Calculations have been performed using different prescriptions for the moment of inertia, $\Im$: $\Im$ independent of the angular momentum, $\Im$ dependent on the angular momentum according to the rotating liquid drop model [19], and $\Im$ corresponding to a superdeformed yrast line crossing the spherical one at an angular momentum $J=28\hbar$ taken from studies of superdeformed bands in this mass region [20–23]. The last two prescriptions are shown in Fig. 3(c) and Fig. 3(d), respectively, and are compared to the experimental spectra. As can be seen, all these calculations do not allow us to reproduce well the alpha particle spectra. A better agreement for protons is obtained, compared to the standard calculation; however, the latter still provides the best overall agreement for all the channels. We conclude that the disagreement found for the $p\alpha$ channel might be related to the treatment of the level density at high angular momenta [24].

In order to get more insight into the CN decay mechanism, the SM predictions with standard parameters have been compared to the measured energy distribution of the entry states (Fig. 4). We observe that the calculated distribution is slightly shifted to higher energy, this being consistent with the findings of Fig. 3(a).

We carried out an analysis of the particle energy spectra, selecting different windows (5 MeV width) of the entry-state energy distribution. These spectra, in the center-of-mass system, are shown in Fig. 5 for both particles and compared with the calculated ones. We note the strong variation of the spectral shapes as a function of the excitation energy. The alpha particle spectra, corresponding to the lower E_f values, differ significantly from the usual Maxwellian shape. This behavior is accounted for by the model which provides the same spectral shapes, although it does not reproduce the relative intensities. Considering that we are dealing with very exclusive data, the ability of the simulation to reproduce well the shapes is surprising. In addition, we observe that for increasing values of E_f, the measured mean proton energy remains almost constant while that of alpha particles decreases. This behavior reveals a different role of the two particles in the energy sharing. The most probable particle energy as a function of E_f is reported in Fig. 6 and compared to the calculated one. The statistical model reproduces the observed behavior: the proton energy remains almost constant while the alpha particle energy decreases as E_f increases. A further test of the SM is provided by the comparison with the measured proton-alpha particle angular correlations shown in Fig. 7 for four E_f windows. The data

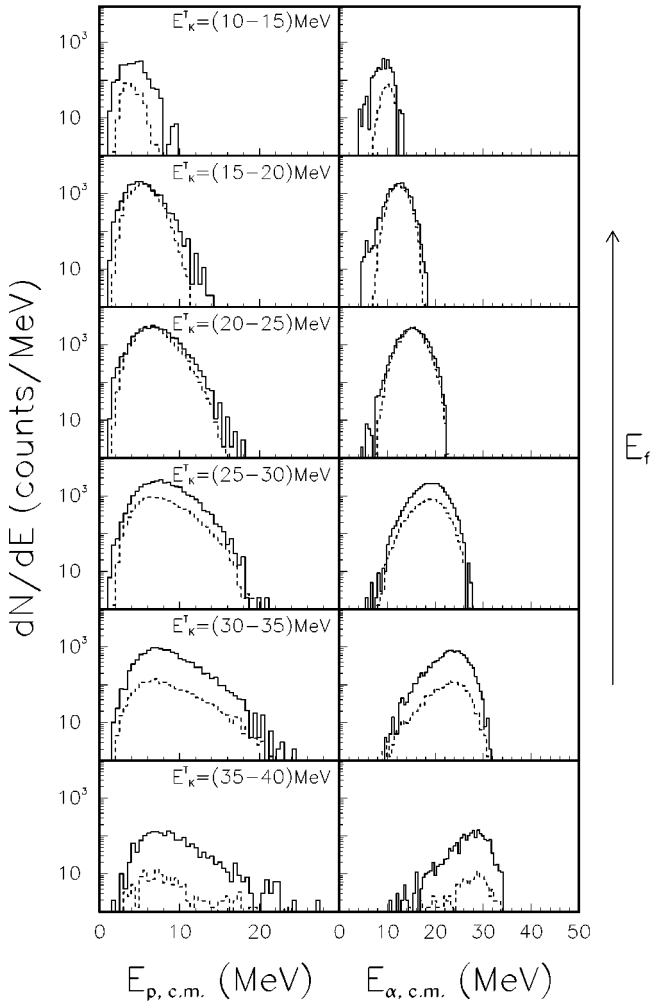

FIG. 5. Measured (solid line) and calculated (dashed line) center-of-mass energy spectra of protons and alpha particles in the $p\alpha$ channel for different residual nucleus (^{85}Nb) excitation energies E_f. The corresponding slices in the total kinetic energy E_K^T are indicated in the figure. Calculated spectra have been normalized to the measured ones at E_K^T=20–25 MeV.

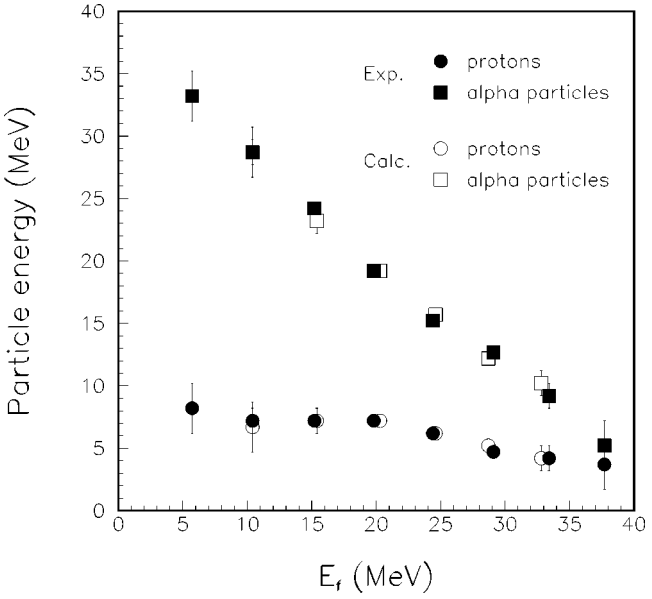

FIG. 6. Most probable energies of the evaporated particles vs the evaporation residue excitation energy E_f in the $p\alpha$ channel.

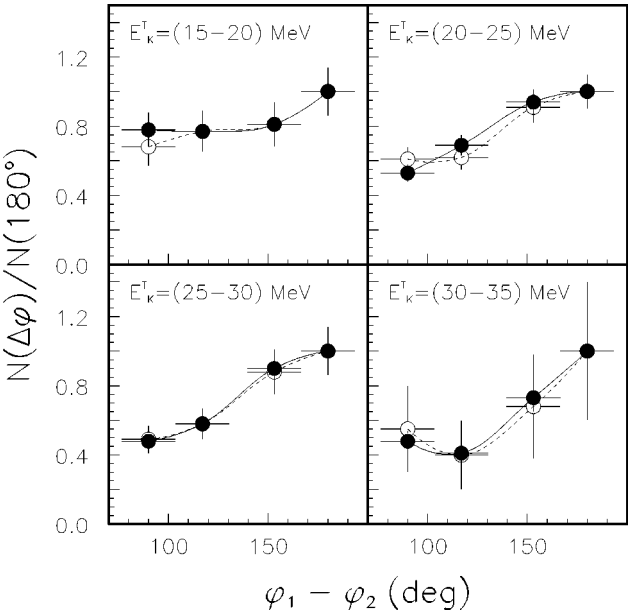

FIG. 7. Measured (solid circles) and calculated (open circles) proton-alpha particle angular correlations for four windows in the excitation energy of the ^{85}Nb evaporation residue, at $\theta_{\rm lab}$=57.5°. Lines are drawn to guide the eye.

are reproduced well by the model. In conclusion, the SM is able to reproduce the spectral shapes and proton-alpha particle angular correlations for this selected channel, making us confident in the predictions of the model. On these grounds we have calculated by the code LILITA_N95 the leading physical quantities involved in the decay. The results are reported in Table II for different intervals of the entry-state excitation energy. In the first three columns, the excitation energy intervals, the corresponding number of events, and the average values of the angular momenta of the compound nucleus are reported. In columns 4 and 5, the average and the widths [full widths at half maximum (FWHM)] of the angular momentum distributions for the entry states are given. The average energies of the emitted particles are reported in columns 6 and 7. In columns 8 and 9 the widths of the proton ($\Delta\theta_p$) and alpha particle ($\Delta\theta_\alpha$) angular distributions with respect to the CN spin direction are presented. These distributions are peaked around 90°. Finally, the alpha particle and proton orbital angular momenta are reported in columns 10 and 11.

The code predicts that the $p\alpha$ channel depopulates high spin states of the compound nucleus, as expected, without correlation to the residual excitation energy. At the same time, a strong correlation between the excitation energy E_f and the angular momentum J_f of the entry states is predicted. The relatively small widths of the angular momentum distributions in the residual nucleus reflect the fact that the entry states are populated in a region of the (E_f, J_f) plane which is relatively narrow and nearly parallel to the yrast line as shown in Fig. 8 where the initial angular momemtum distribution is also shown. This behavior is due to the relatively small thermal energy available to the decay of high spin states of the CN. Because of this constraint, imposed by the yrast line, particles with high kinetic energy are evaporated by the CN mainly at the expense of its rotational energy, thus carrying away a large amount af angular momentum. In this picture we can understand the observed behavior in the energy sharing between protons and alpha particles. Alpha particles are able to take away most of the available excitation

TABLE II. Calculated quantities characterizing the $p\alpha$ decay of the ^{90}Ru compound nucleus. In the first three columns the excitation energy intervals, the corresponding number of events, and the average values of the angular momenta of the compound nucleus are reported. In columns 4 and 5, the average and the width (FWHM) of the angular momentum distributions of the evaporation residue are given. The average energies of the emitted particles are reported in columns 6 and 7. In the columns 8 and 9 the widths of the proton and alpha particle angular distributions with respect to the CN spin direction are presented. Finally, the alpha particle and proton orbital angular momenta are given in columns 10 and 11.

E_f (MeV)	N	$J_{\rm CN}$ ($\hbar$)	J_f ($\hbar$)	ΔJ_f ($\hbar$)	E_α (MeV)	E_p (MeV)	$\Delta\theta_\alpha$ (deg)	$\Delta\theta_p$ (deg)	l_α ($\hbar$)	l_p ($\hbar$)
(12.5–17.5)	393	33.0	22.6	4.0	21.4	8.2	43	67	10.8	1.9
(17.5–22.5)	1023	33.6	25.5	3.5	17.5	7.8	54	67	7.7	1.8
(22.5–27.5)	1116	34.0	30.0	2.8	14.1	6.9	69	70	5.0	1.6
(27.5–32.5)	235	34.4	33.0	2.0	11.7	5.4	87	78	3.1	1.3

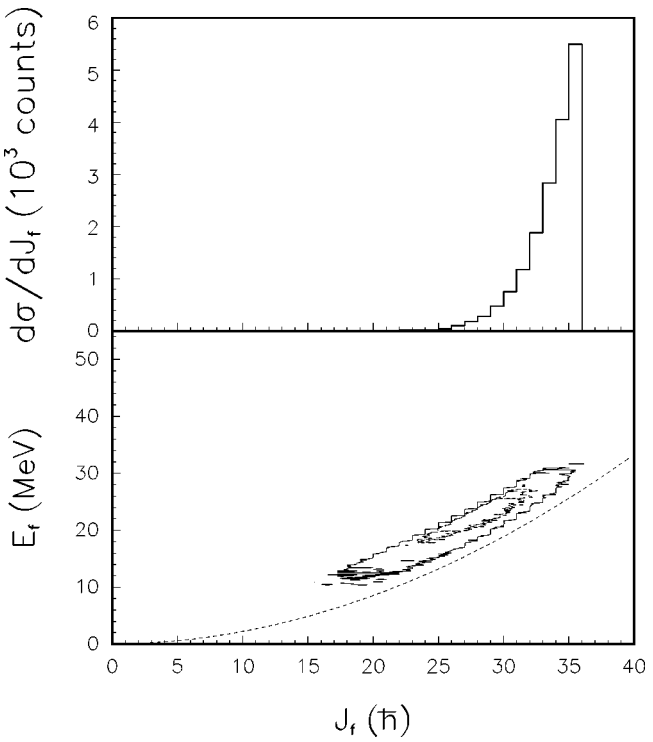

FIG. 8. Lower part: distribution of the residual nucleus ^{85}Nb populated via the $p\alpha$ channel in the (E_f, J_f) plane calculated by the statistical code LILITA_N95. Contour values are 3 (solid line) and 30 (dashed line). The yrast line of the residual nucleus assuming a rigid sphere is also shown. Upper part: calculated CN spin distribution relative to the deexcitation via the $p\alpha$ channel.

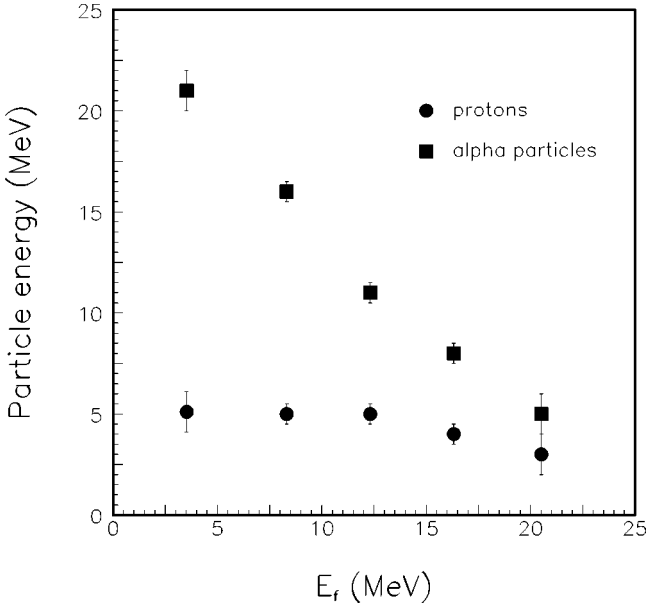

FIG. 9. Measured most probable energies of the evaporated particles vs the evaporation residue excitation energy E_f in the $p\alpha$ channel for the ^{44}Ti compound nucleus.

energy, because of their ability to carry away a larger amount of angular momentum compared to protons. This behavior is predicted by the calculation to be independent of the order of particle emission. Furthermore, as expected, higher particle energies correspond to lower values of $\Delta\theta_\alpha$, indicating a higher degree of angular momentum alignment between the compound nucleus and the alpha particle. This effect is predicted to be small for protons as shown by the variations of $\Delta\theta_p$ as a function of E_f. From the experimental point of view, this behavior is manifested by the measured proton-alpha particle angular correlations shown in Fig. 7. Going to lower values of E_f, the measured and calculated anisotropies increase. This can be ascribed to the enhancement of the spin alignment between the emitters and the particles.

How general is the found behavior in the decay mechanism of the $p\alpha$ channel is a matter of further investigations. A similar study on the $p\alpha$ decay channel has been carried out on the lighter ^{44}Ti CN. This was produced by the 50 MeV ^{16}O + ^{28}Si reaction [5], at 43.1 MeV excitation energy and $22\hbar$ maximum angular momentum. We observed a similar behavior in the sharing of the available energy between the two particles as shown in Fig. 9 where the measured most probable energies of protons and alpha particles, as a function of E_f, are presented.

IV. CONCLUSION

The light charged-particle detector DIAMANT coupled to the γ-ray spectrometer EUROGAM II has been used to study the decay of the ^{90}Ru compound nucleus. The high efficiency of the apparatus allowed us a detailed study of the $p\alpha$ channel produced with $\simeq 1\%$ of the fusion cross section. The proton and alpha particle energy spectra as a function of the excitation energy of the entry states have been extracted. We observe an interesting behavior in the sharing of the available energy between the two particles: as the excitation energy of the evaporation residue decreases, the proton energy remains almost constant while the alpha particles carry away the remaining energy. Similar results have been found for the decay of the ^{44}Ti compound nucleus. This behavior could be observed for the first time due to the high selectivity of the apparatus. From the theoretical point of view the SM proved to be able to reproduce the main features of the exclusive data. The decay seems to be governed by the constraints imposed by the yrast line at high angular momenta, resulting in a strong predicted correlation between the excitation energy and the angular momentum of the residual nucleus. This correlation encourages the use of the $p\alpha$ decay channel to enhance the observability of superdeformed bands selecting the entry states of the residual nucleus by the energies of the emitted particles.

ACKNOWLEDGMENTS

The authors acknowledge the valuable assistance given during the experiment by the staff of the EUROGAM spectrometer and of the VIVITRON accelerator in Strasbourg. This work has been supported in part by IN2P3, Region Aquitaine, INFN, and by the EC under HCM network Contract Nos. ERBCHRXCT 930367 and 930364.

[1] W.E. Parker, M. Kaplan, D.J. Moses, G. La Rana, D. Logan, R. Lacey, J.M. Alexander, D.M. de Castro Rizzo, P. DeYoung, R.J. Welberry, and J.T. Boger, Phys. Rev. C **44**, 774 (1991), and references therein.

[2] S. Henss, A. Ruckelshausen, R.D. Fischer, W. Kühn, V. Metag, R. Novotny, R.V.F. Janssens, T.L. Khoo, D. Habs, D. Schwalm, D. Freeman, G. Duchène, B. Haas, F. Haas, S. Hlavac, and R.S. Simon, Phys. Rev. Lett. **60**, 11 (1988).

[3] M. Lunardon, G. Viesti, D. Bazzacco, R. Burch, D. Fabris, S. Lunardi, N. Medina, G. Nebbia, C. Rossi-Alvarez, G. de Angelis, M. De Poli, E. Fioretto, G. Prete, J. Rico, P. Spolaore, G. Vedovato, A. Brondi, G. La Rana, R. Moro, and E. Vardaci, Nucl. Phys. **A583**, 215 (1995).

[4] J.-N. Scheurer, M.-M. Aleonard, G. Barreau, F. Bourgine, J.-F. Chemin, T.P. Doan, D. Sellam, A. Brondi, G. La Rana, R. Moro, E. Vardaci, F. Hannachi, and D. Curien, in *Proceedings of the International Conference on the Future of Nuclear Spectroscopy*, Crete, 1993, edited by W. Gelletly *et al.* (NCSR Demokritos, Athens, 1994), p. 371.

[5] D. Cabaussel, Ph.D. thesis, University of Bordeaux, France, 1996.

[6] ''EUROGAM,'' Internal EUROGAM Collaboration Report, CRN Strasbourg, 1990.

[7] G.J. Gross, K.P. Lieb, D. Rudolph, M.A. Bentley, W. Gelletly, H.G. Price, J. Simpson, D.J. Blumenthal, P.J. Ennis, C.J. Lister, Ch. Winter, J.L. Durell, B.J. Varley, Ö. Skeppstedt, and S. Rastikerdar, Nucl. Phys. **A535**, 203 (1991).

[8] J.-N. Scheurer, M. Aïche, M.-M. Aleonard, G. Barreau, F. Bourgine, D. Boivin, D. Cabaussel, J.-F. Chemin, T.P. Doan, M. Harston, A. Brondi, G. La Rana, R. Moro, E. Vardaci, and D. Curien, Nucl. Instrum. Methods Phys. Res. A **385**, 501 (1997).

[9] M. Aïche, M.-M. Aleonard, G. Barreau, F. Bourgine, D. Boivin, D. Cabaussel, J.-F. Chemin, T.P. Doan, M. Harston, J.-N. Scheurer, A. Brondi, G. La Rana, R. Moro, E. Vardaci, and D. Curien, Nucl. Instrum. Methods Phys. Res. A (submitted).

[10] D.G. Sarantites, C. Baktash, N.G. Nicolis, G. Garcia-Bermudez, V. Abenante, J.R. Beene, N.R. Johnson, M.L. Halbert, D.C. Hensley, F.K. McGowan, H.C. Griffin, I.Y. Lee, Z. Majka, M.A. Riley, T.M. Semkow, D.C. Stracener, and A. Virtanen, Phys. Rev. Lett. **64**, 2129 (1990).

[11] D.J. Blumenthal, C.J. Lister, P. Chowdhury, B. Crowell, P.J. Ennis, Ch. Winter, T. Drake, A. Galindo-Uribarri, G. Zwartz, H.R. Andrews, G.C. Ball, D. Radford, D. Ward, and V.P. Janzen, Phys. Rev. Lett. **66**, 3121 (1991).

[12] G. Viesti, M. Lunardon, D. Bazzacco, R. Burch, D. Fabris, S. Lunardi, N.H. Medina, G. Nebbia, C. Rossi Alvarez, G. de Angelis, M. Cinausero, E. Farnea, E. Fioretto, G. Prete, and G. Vedovato, Phys. Lett. B **382**, 24 (1996).

[13] P.O. Tjøm, I. Espe, G.B. Hagemann, B. Herskind, and D.L. Hillis, Phys. Lett. **72B**, 439 (1978).

[14] D.G. Sarantites, R. Lovett, and R. Woodward, Nucl. Instrum. Methods **171**, 503 (1980).

[15] M. Jääskeläinen, D.G. Sarantites, R. Woodward, F.A. Dilmanian, J.T. Hood, R. Jääskeläinen, D.C. Hensley, M.L. Halbert, and J.H. Barker, Nucl. Instrum. Methods Phys. Res. **204**, 385 (1983).

[16] A.M. Stefanini, G. Fortuna, R. Pengo, W. Meczynski, G. Montagnoli, L. Corradi, A. Tivelli, S. Beghini, C. Signorini, S. Lunardi, M. Morando, and F. Soramel, Nucl. Phys. **A456**, 509 (1986).

[17] The code LILITA_N95 is an extensively modified version of the LILITA program originally developed by J. Gomez del Campo and R.G. Stokstad [25]. It has been renamed to differentiate it from several other versions of LILITA.

[18] The potentials used to calculate optical model transmission coefficients are from D. Wilmore and P.E. Hodgson, Nucl. Phys. **55**, 673 (1964) for neutrons; C.M. Perey and F.G. Perey, Nucl. Data, Sect. B **10**, 539 (1972) for protons; J.R. Huizenga and G. Igo, Nucl. Phys. **29**, 462 (1962) for alpha particles.

[19] J.R. Huizenga, A.N. Behkami, I.M. Govil, W.U. Schröder, and J. Tõke, Phys. Rev. C **40**, 668 (1989).

[20] C. Baktash, D.M. Cullen, J.D. Garrett, C.J. Gross, N.R. Johnson, W. Nazarewicz, D.G. Sarantites, J. Simpson, and T.R. Werner, Phys. Rev. Lett. **74**, 1946 (1995).

[21] A.G. Smith, P.J. Dagnall, J.C. Lisle, D.H. Smalley, T.R. Werner, R. Chapman, C. Finck, B. Haas, M. Leddy, W. Nazarewicz, D. Prévost, N. Rowley, and H. Savajols, Phys. Lett. B **355**, 32 (1995).

[22] H.-Q. Jin, C. Baktash, M.J. Brinkman, C.J. Gross, D.G. Sarantites, I.Y. Lee, B. Cederwall, F. Cristancho, J. Döring, F.E. Durham, P.-F. Hua, G.D. Johns, M. Korolija, D.R. LaFosse, E. Landulfo, A.O. Macchiavelli, W. Rathbun, J.X. Saladin, D.W. Stracener, S.L. Tabor, and T.R. Werner, Phys. Rev. Lett. **75**, 1471 (1995).

[23] P.J. Dagnall, A.G. Smith, J.C. Lisle, D.H. Smalley, R. Chapman, C. Finck, B. Haas, M. Leddy, D. Prévost, N. Rowley, and H. Savajols, Z. Phys. A **353**, 251 (1995).

[24] S. Åberg, Nucl. Phys. **A477**, 18 (1988).

[25] J. Gomez del Campo and R.G. Stokstad, ONRL report, 1981.